U.S. National Library of Medicine
National Center for Biotechnology Information

NLM Citation: Zhang H. Hyperpolarized sodium 1-[^{13}C]pyruvate. 2008 Jan 29 [Updated 2008 Feb 28]. In: Molecular Imaging and Contrast Agent Database (MICAD) [Internet]. Bethesda (MD): National Center for Biotechnology Information (US); 2004-2013.
Bookshelf URL: https://www.ncbi.nlm.nih.gov/books/

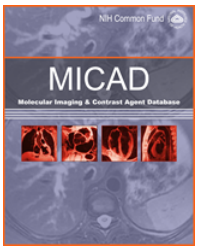

Hyperpolarized sodium 1-[^{13}C]pyruvate

HP[^{13}C]Pyr

Huiming Zhang, PhD[1]

Created: January 29, 2008; Updated: February 28, 2008.

Chemical name:	Hyperpolarized sodium 1-[^{13}C]pyruvate
Abbreviated name:	HP[^{13}C]Pyr
Synonym:	Sodium pyruvate-1-^{13}C, Pyruvic acid-1-^{13}C sodium
Agent category:	Small molecule
Target:	Other
Target category:	Other -metabolism
Method of detection:	Magnetic resonance spectroscopic imaging (MRSI), magnetic resonance imaging (MRI)
Source of signal/ contrast:	^{13}C
Activation:	No
Studies:	• *In vitro* • Rodents

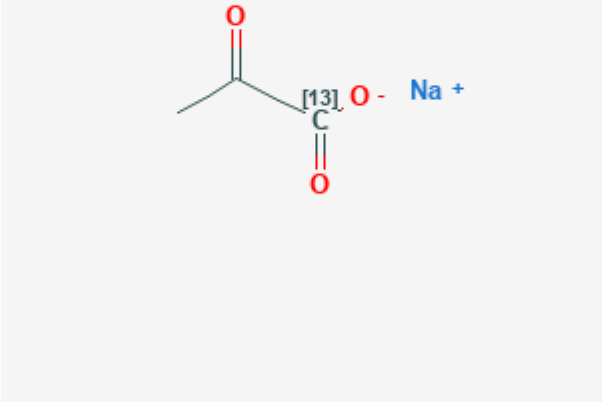

Click on the above structure for additional information in PubChem.

Background

[PubMed]

Pyruvate (Pyr) is an endogenous substrate enriched at a crossroad of the major energy-generating metabolic pathways in mammalian cells (1). Under most physiological conditions, the bulk of intracellular Pyr is generated endogenously by glycolysis of glucose or oxidation of lactate (Lac) (2). Pyr is then converted into several products through different metabolic pathways in mitochondria or cytoplasm (2, 3). In mitochondria, one of the major pathways is the irreversible transformation of Pyr into acetyl-coenzyme A (acetyl-CoA) and CO_2 by pyruvate dehydrogenase (PDH) in the presence of coenzyme nicotinamide adenine dinucleotide (NAD^+/ NADH). Another major pathway is the conversion of Pyr into oxaloacetate by PDH. Both acetyl-CoA and oxaloacetate are substrates of the tricarboxylic acid cycle (TCA), also known as the Krebs cycle, which generates

Author Affiliation: 1 National Center for Biotechnology Information, NLM, NIH, Bethesda, MD; Email: micad@ncbi.nlm.nih.gov.

adenosine triphosphate (ATP) and provides energy to the cell. In the cytoplasm, Pyr is converted into alanine (Ala) by glutamine-Pyr transaminase (GPT) and reversibly oxidized back to Lac by lactate dehydrogenase (LDH). With its ability to increase cardiac mechanical performance and energy reserves, Pyr has been an important therapeutic agent in the treatment of diseases such as dysfunctional myocardium (2). Pyr is also a diagnostic marker in cancers because it is abundantly converted to Lac through anaerobic glycolysis (1). The abnormality of Pyr metabolism in diseased tissue can be detected through quantification of its metabolites. ^{13}C Magnetic resonance spectroscopic imaging (MRSI) is suitable for *in vivo* quantification because of the inherent chemical shift dispersion of the major metabolites of Pyr (4). The chemical shift value is 178 ppm for Ala, 185 ppm for Lac, 124.5 ppm for CO_2, and 173 ppm for Pyr itself (4). Since ^{13}C has low natural abundance (1.1%) and a low gyromagnetic ratio (one quarter compared to proton spin), direct measurement of these metabolites is extremely difficult even with high magnetic fields. The recently developed hyperpolarization technique can increase the signal/noise ratio (SNR) by 10,000-fold (5), allowing direct detection of these metabolites *via* ^{13}C MRSI.

The signal of nuclear magnetic resonance (NMR) imaging is proportional to the thermal equilibrium polarization of nuclear spins. As a function of magnetic field strength and temperature, the thermal equilibrium polarization normally is very low (i.e., 1×10^{-6} for ^{13}C at 1.5 T and at body temperature). The hyperpolarization technique increases the polarization of spins by creating an artificial, non-equilibrium distribution of nuclei. Dynamic nuclear polarization (DNP) is an effective technique to hyperpolarize the ^{13}C nuclei of Pyr. Electron spins have a large magnetic moment that is ~660 times stronger than the magnetic moment of proton spins. This strong magnetic moment can be transferred to proton spins through the DNP technique. Theoretically, the DNP enhancement factor for NMR signals depends on the ratio of the electronic gyromagnetic ratio to the nuclear gyromagnetic ratio (γ_e/γ_n) in high magnetic fields, which corresponds to a DNP enhancement factor of ~660 for ^{1}H nuclei and ~2600 for ^{13}C nuclei (6). There are four mechanisms accounted for in the DNP process: the Overhauser effect, the solid effect, thermal mixing, and the cross effect or electronuclear cross-polarization (7). The DNP experiments are generally conducted at low temperatures to attenuate competing spin-lattice relaxation processes and avoid loss of efficiency during the polarization transfer (9). Radicals containing unpaired electrons, which have a thermal equilibrium polarization of almost unity when exposed to a magnetic field of ~3 T at a temperature of ~1 K, are added (8). Microwave irradiation near the electron resonance frequency of the radical is used to transfer the polarization from the unpaired electrons on the radicals to the ^{13}C nuclei on substrates. As a result of the short T_1 of the electrons (~1 μs), the electrons rapidly regain their polarization. This continuous pumping process can increase the nuclear polarization in the solid material by 20–40% (8). By rapid dissolution, the solid is transformed into an injectable liquid with small polarization losses. The use of DNP produces an enhancement factor of 10^5 in ^{13}C polarization compared to the thermal equilibrium state at typical magnetic field strengths (8), allowing for direct imaging of metabolites at mM *in vivo*.

A major difference between the signal of hyperpolarized ^{13}C and the signal of conventional NMR is that the magnetization of hyperpolarized ^{13}C is created outside the magnetic field in a polarizer system (9). Once the hyperpolarization has been created, the polarization will strive to return to the thermal equilibrium level at a rate governed by T_1 relaxation time, which typically ranges from a few seconds to several minutes for ^{13}C. The corresponding time window for imaging is approximately a few minutes. Because the 1.1% natural abundance of ^{13}C produces a negligible ^{13}C signal, there is virtually no background signal other than noise from the patient and the coil/receiver system. The injected hyperpolarized ^{13}C-labeled Pyr (HP[^{13}C]Pyr) generates a ^{13}C signal that is linearly proportional to its concentration. In this respect, hyperpolarized ^{13}C MRI behaves in a manner similar to modalities such as positron emission tomography (PET) and single-photon emission tomography (SPECT). Neither PET nor SPECT can distinguish between metabolites and substrates. However, the large chemical shift dispersion in ^{13}C MRSI can be used for quantification of each metabolite (10). The measurement of spatial distribution of metabolites *via* ^{13}C MRSI allows the establishment of enzyme activity maps (11).

Synthesis

[PubMed]

The preparation of HP[^{13}C]Pyr was described by several authors (10, 12). Two starting materials, [1-^{13}C]Pyr and Tris{8-carboxyl-2,2,6,6-tetra[2-(1-hydroxyethyl)]-benzo(1,2-d:4,5-d')bis(1,3)dithiole-4-yl}methyl sodium (trityl radical), were commercially available. Both chemicals were dissolved in an aqueous solvent and loaded into a chamber where the sample was cooled to 1.2 K at a pressure of 0.8 mbar. The sample was then irradiated with microwaves (~93.9 GHz) in a helium bath at a magnetic field of 3.35 T for >1 h. After the polarization, the sample was dissolved with hot solvents to produce an injectable solution at approximately 37°C. The level of polarization was estimated by measuring the free induction decays of an aliquot in a NMR spectrometer. The typical polarization was 20–30%.

In Vitro Studies: Testing in Cells and Tissues

[PubMed]

The evaluation of HP[^{13}C]Pyr influx in EL-4 mouse lymphoma cells was conducted with a 9.4-T imager (11). After adding HP[^{13}C]Pyr into the cells, the conversion of Pyr to Lac produced an increased Lac carboxyl signal that decayed at an apparent T_1 of 40 s. The ^{13}C peak intensities for Pyr and Lac were fitted to a modified two-site exchange Bloch equation to extract the apparent exchange rate constants. These rate constants were used to evaluate the LDH activity and Pyr influx during drug treatment. Etoposide was an inhibitor of the enzyme topoisomerase II used in chemotherapy for various malignant carcinomas. A 16-h treatment of the tumor cells with etoposide caused ~30–40% apoptosis and 10–15% necrosis in the cells. This induced ~80% reduction in Pyr flux, which was decreased from 54 ± 15 nmol/s per 10^8 cells to 9.0 ± 1.5 nmol/s per 10^8 cells. The LDH activity was nearly the same: 5.43 ± 0.34 units/10^7 cells in control cells and 5.37 ± 0.27 units/10^7 cells in drug-treated cells. A 20-h treatment with etoposide produced a 45% necrosis in the cells. The LDH activity also decreased significantly to 2.53 ± 0.32 units/10^7 cells. The levels of necrosis and apoptosis were further confirmed by flow cytometry.

The metabolism of HP[^{13}C]Pyr in isolated rat hearts was examined at 14.1 T (10). Hearts from adult rats were rapidly excised and perfused at 37°C using standard Langendorff methods. After each aorta was cannulated, each heart was placed in a NMR tube that was then filled with recirculated medium containing fatty acids and 2 mM HP[^{13}C]Pyr with 20–30% polarization. Fatty acids with even or odd carbons were used to modulate the influx of PDH. Propionate (a three-carbon fatty acid) activated 90% PDH and stimulated PDH flux, whereas even-carbon fatty acid strongly inhibited PDH. Experiments were performed under ideal conditions for detected downstream metabolites such as $H^{13}CO_3^-$ (160.9 ppm) and $^{13}CO_2$ (124.5 ppm) in the presence of HP[^{13}C]Pyr alone as well as in the presence of HP[^{13}C]Pyr with even or odd fatty acids. The intensity of the $H^{13}CO_3^-$ and $^{13}CO_2$ resonances in the hearts reached a maximum of ~20 s after infusion of HP[^{13}C]Pyr. The ratio of the $H^{13}CO_3^-$ resonance area to the $^{13}CO_2$ area was 7.03 ± 0.5 and remained constant until T_1 relaxation began to destroy the $^{13}CO_2$ signal. In the presence of octanoate, a medium chain fatty acid, $H^{13}CO_3^-$ and $^{13}CO_2$ were nearly invisible and did not recover even in the presence of propionate. This result suggested an effective competition of octanoate with Pyr for supplying acetyl-CoA to the heart.

Animal Studies

Rodents

[PubMed]

The dynamic spectra of HP[^{13}C]Pyr were collected in rats at 3 T (4). Healthy rats were injected intravenously with 3 ml of HP[^{13}C]Pyr solution at 79 mM in 12 s. Chemical shift imaging (CSI) of a thick slab was initiated ~30 s after the injection of HP[^{13}C]Pyr with a dual-tuned volume coil was started, and the CSI were acquired every 3 s. The produced images for a 90-mm slab reflected a combined effect of metabolism, blood flow, and T_1 relaxation. The results demonstrated that the conversion of Pyr to its metabolites, including Lac, Ala, and bicarbonate, occurred within a minute of injection. Among these metabolites, Ala was observed primarily in skeletal muscle and liver; Lac and bicarbonate were relatively concentrated in the vasculature and kidneys.

The metabolism of HP[^{13}C]Pyr in lymphoma tumors was examined in mice at 9.4 T (11). After intravenous injection of 0.2 ml of HP[^{13}C]Pyr solution at 75 mM within 3 s, ^{13}C magnetic resonance spectroscopy (MRS) and ^{13}C MRSI were used to evaluate the flux between Pyr and Lac in the tumors. A series of images was acquired to calculate an enzyme activity map. The experiments were performed in mice with and without etoposide treatment. There was a substantial signal from Pyr but only a small signal from Lac in drug-treated and untreated mice. The signal intensities were fitted to a two-site exchange Bloch equation to extract apparent exchange rate constants and spin-lattice relaxation times. A treatment with etoposide resulted in 37 ± 4% death of tumors *versus* 5 ± 1% in the control group. This led to ~25% reduction in the rate constant of Pyr, which decreased from 0.075 ± 0.011 s^{-1} to 0.056 ± 0.005 s^{-1}. The decreased flux between Pyr and Lac were demonstrated in a plot in terms of the labeled Lac/Pyr ratio. Pyr concentration in excised tumors was 0.55 ± 0.19 μmol/g in control tumors and 0.75 ± 0.48 μmol/g in drug-treated tumors as determined by ^{1}H NMR.

The metabolism of HP[^{13}C]Pyr was also examined in P22 tumors implanted in six rats (1). ^{13}C-Labeled CSI images were collected for a slice 10 mm thick with a 5×5-mm^2 in-plane pixel size at 1.5 T. HP[^{13}C]Pyr was infused in 14 s at a dose of 0.79 mmol/kg. The ^{13}C CSI scans were acquired starting 30 s after the infusion began. All tumors showed significantly higher Lac content within 30 s than the normal tissue. The metabolic conversion of Pyr into Ala and Lac was found in all rats, but the Lac production was especially pronounced in all the tumors. HP[^{13}C]Pyr was used to evaluate the Lac production in transgenic adenocarcinomas of mouse prostate (TRAMP) mice at 3 T (12). ^{13}C MRI or ^{13}C MRSI were collected for both primary and metastatic tumors. The primary tumors and lymph node metastases showed much higher Lac levels compared to the normal mouse prostates.

Other Non-Primate Mammals

[PubMed]

No publication is currently available.

Non-Human Primates

[PubMed]

No publication is currently available.

Human Studies

[PubMed]

No publication is currently available.

NIH Support

RR 02584, HL 34557, EB005363, EB007588

References

1. Golman K., Zandt R.I., Lerche M., Pehrson R., Ardenkjaer-Larsen J.H. Metabolic imaging by hyperpolarized 13C magnetic resonance imaging for in vivo tumor diagnosis. Cancer Res. 2006; **66** (22):10855–60. PubMed PMID: 17108122.
2. Mallet R.T. Pyruvate: metabolic protector of cardiac performance. Proc Soc Exp Biol Med. 2000; **223** (2):136–48. PubMed PMID: 10654616.
3. Koukourakis M.I., Giatromanolaki A., Sivridis E., Gatter K.C., Harris A.L. Pyruvate dehydrogenase and pyruvate dehydrogenase kinase expression in non small cell lung cancer and tumor-associated stroma. Neoplasia. 2005; **7** (1):1–6. PubMed PMID: 15736311.
4. Kohler S.J., Yen Y., Wolber J., Chen A.P., Albers M.J., Bok R., Zhang V., Tropp J., Nelson S., Vigneron D.B., Kurhanewicz J., Hurd R.E. In vivo 13 carbon metabolic imaging at 3T with hyperpolarized 13C-1-pyruvate. Magn Reson Med. 2007; **58** (1):65–9. PubMed PMID: 17659629.
5. Ardenkjaer-Larsen J.H., Fridlund B., Gram A., Hansson G., Hansson L., Lerche M.H., Servin R., Thaning M., Golman K. Increase in signal-to-noise ratio of > 10,000 times in liquid-state NMR. Proc Natl Acad Sci U S A. 2003; **100** (18):10158–63. PubMed PMID: 12930897.
6. Hall D.A., Maus D.C., Gerfen G.J., Inati S.J., Becerra L.R., Dahlquist F.W., Griffin R.G. Polarization-enhanced NMR spectroscopy of biomolecules in frozen solution. Science. 1997; **276** (5314):930–2. PubMed PMID: 9139651.
7. Joo C.G., Hu K.N., Bryant J.A., Griffin R.G. In situ temperature jump high-frequency dynamic nuclear polarization experiments: enhanced sensitivity in liquid-state NMR spectroscopy. J Am Chem Soc. 2006; **128** (29):9428–32. PubMed PMID: 16848479.
8. Mansson S., Johansson E., Magnusson P., Chai C.M., Hansson G., Petersson J.S., Stahlberg F., Golman K. 13C imaging-a new diagnostic platform. Eur Radiol. 2006; **16** (1):57–67. PubMed PMID: 16402256.
9. Olsson L.E., Chai C.M., Axelsson O., Karlsson M., Golman K., Petersson J.S. MR coronary angiography in pigs with intraarterial injections of a hyperpolarized 13C substance. Magn Reson Med. 2006; **55** (4):731–7. PubMed PMID: 16538605.
10. Merritt M.E., Harrison C., Storey C., Jeffrey F.M., Sherry A.D., Malloy C.R. Hyperpolarized 13C allows a direct measure of flux through a single enzyme-catalyzed step by NMR. Proc Natl Acad Sci U S A. 2007; **104** (50):19773–7. PubMed PMID: 18056642.
11. Day S.E., Kettunen M.I., Gallagher F.A., Hu D.E., Lerche M., Wolber J., Golman K., Ardenkjaer-Larsen J.H., Brindle K.M. Detecting tumor response to treatment using hyperpolarized 13C magnetic resonance imaging and spectroscopy. Nat Med. 2007; **13** (11):1382–7. PubMed PMID: 17965722.
12. Chen A.P., Albers M.J., Cunningham C.H., Kohler S.J., Yen Y.F., Hurd R.E., Tropp J., Bok R., Pauly J.M., Nelson S.J., Kurhanewicz J., Vigneron D.B. Hyperpolarized C-13 spectroscopic imaging of the TRAMP mouse at 3T-initial experience. Magn Reson Med. 2007; **58** (6):1099–106. PubMed PMID: 17969006.